

Dilatometric Analysis of Phase Fraction during Austenite Decomposition into Banded Microstructure in Low-Carbon Steel

DONG-WOO SUH, CHANG-SEOK OH, HEUNG NAM HAN, and SUNG-JOON KIM

The evolution of microstructural bands in low-carbon steel gives rise to the orientation dependence of dilatation behavior, which is associated with a distinct, specimen-orientation-dependent, nonisotropic dilatation. In this article, the authors attempt to analyze the phase fraction from the dilatometric curve, which shows orientation dependence due to the effect of microstructural directionality. The contribution of nonisotropic dilatation to the observed dilatation behavior is quantified and integrated into the analysis procedure by considering its evolution from the microstructural and the geometric effects. The proposed dilatometric analysis is applied to the evaluation of the phase fraction during austenite decomposition into a banded microstructure in a low-carbon steel. From dissimilar dilatometric curves measured along different specimen orientations, the phase fractions involved with the austenite decomposition can be consistently evaluated with the proposed analysis procedure. The analysis results are also in agreement with the metallographically analyzed ones.

DOI: 10.1007/s11661-007-9361-9

© The Minerals, Metals & Materials Society and ASM International 2007

I. INTRODUCTION

DILATOMETRIC curves of carbon steels exhibit characteristic changes during the phase transformation on thermal cycles due to the difference of atomic volume among the phases involved in the transformation. Many dilatometric analysis models have been proposed to extract the phase fractions from the dilatometric curve, including the lever rule and other analysis methods considering the carbon enrichment in austenite.^[1–11] Recently, the authors suggested an analysis model that could further take into account the nonisotropic volume change during the transformation.^[12]

For the evaluation of the phase fraction, most of the previous dilatometric studies employed a dilatometric curve that was measured along a single specimen orientation, assuming that the dilatometric analysis would yield almost the same results regardless of the measured orientation. Those approaches are reasonable when the specimen has a homogeneous microstructure and thus exhibits similar dilatation behaviors for any orientation. However, it is not clear that they still give reliable results when the material shows distinctly different dilatation behavior depending on the specimen orientation.

Microstructural bands, which refer to the alternating layers of ferrite and second phase, are commonly observed in hot-rolled, low-carbon steels. The segrega-

tion of substitutional alloying elements during solidification and the elongation of the segregated region during hot rolling are known to be responsible for their development.^[13,14] It was reported that the microstructural bands had a detrimental effect on toughness properties as a result of orientation-dependent impact energy.^[15] Recent investigations revealed that the dilatation behavior of low-carbon steels varied with the specimen orientation when the microstructural bands evolved during the transformation.^[16–18] It was confirmed that the orientation dependence of dilatometric curves was associated with the microstructural directionality. However, it has been rarely investigated whether the conventional dilatometric analysis could provide reliable phase fractions from the dilatometric curves varying with the measured orientation. The study of Kop *et al.*^[16] is probably the only work that reported the dilatometric analysis while taking into account the orientation dependence of dilatometric curves. They attempted to consider the effect of the microstructural directionality by introducing a correction factor for the strain of each constituent phase, even though their approach had difficulties in reflecting quantitatively the physical insight of the phenomenon. Recently, Jaramillo *et al.*^[18] successfully predicted the orientation dependence of the dilatometric curves of carbon steel with an artificial banded layer fabricated by the roll bonding of stacked sheets. Their study is basically intended to model the orientation dependence of the dilatation behavior originating from the microstructural directionality, and the dilatometric analysis for evaluating the phase fractions was not considered.

Since the overall volume change associated with the transformation should be the same under a given thermal cycle, the variation of dilatometric curve with the specimen orientation will be generated by a nonisotropic volume change of the specimen during

DONG-WOO SUH, Senior Researcher, CHANG-SEOK OH, Principal Researcher, and SUNG-JOON KIM, Principal Researcher, are with the Department of Advanced Metallic Materials, Korea Institute of Materials Science, Kyungnam, 641-010 Korea. Contact e-mail: dongwoo@kims.re.kr HEUNG NAM HAN, Assistant Professor, is with the School of Materials Science and Engineering, Seoul National University, Seoul, 151-742 Korea.

Manuscript submitted June 15, 2007.

Article published online October 27, 2007

the transformation. In our previous article,^[12] the contribution of nonisotropic volume change to dilatation data was specified as nonisotropic dilatation, and its effect on the dilatometric analysis was considered for a microstructurally homogeneous specimen. This article proposes a dilatometric analysis procedure for the austenite decomposition of low-carbon steels when the dilatometric curves show orientation dependence due to the microstructural bands. The effect of microstructural directionality on the dilatation behavior is examined and the nonisotropic dilatation originating from the microstructural directionality is considered in the dilatometric analysis. The proposed analysis procedure is applied to the evaluation of the phase fraction during austenite decomposition into a banded microstructure in low-carbon steel, and the validity of the analysis result is discussed.

II. EXPERIMENTAL PROCEDURE AND RESULTS

The chemical composition of investigated steel is listed in Table I. Commercial slab with a thickness of 220 mm was hot-rolled to a plate with a thickness of 20 mm and with a temperature between 1200 °C and 950 °C. The initial microstructure of the hot-rolled plate in Figure 1 clearly shows the microstructural bands parallel to the rolling direction. Cylindrical dilatometric specimens with a dimension of 3 mm (ϕ) \times 10 mm (L) were machined for L direction to be parallel to the banded layer (RD specimen) or perpendicular to it (ND specimen). The dilatometric measurement was performed using a quench dilatometer (DILATRONIC III*),

*Dilatronic III is a trademark of Theta Industries, Inc., Port Washington, NY.

Table I. Chemical Composition of Investigated Steel (Weight Percent)

C	Mn	Si	P	S
0.144	1.1	0.11	0.01	0.006

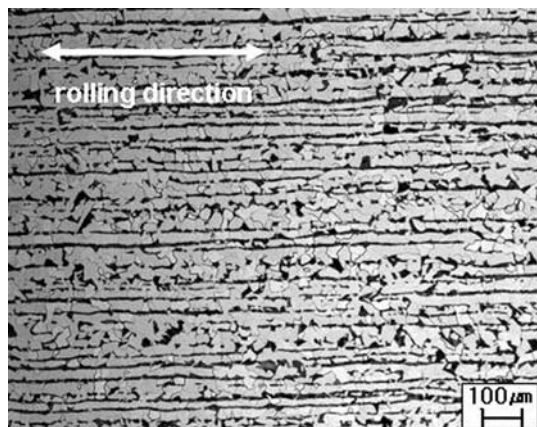


Fig. 1—Initial microstructure of hot-rolled plate.

which heats the specimen with an induction coil and detects the length change along L direction with a linear variable displacement transducer. The temperature of the specimen was monitored with an R-type thermocouple attached to the specimen surface. The dilatometric specimens were heated to 950 °C at the heating rate of 1 °C/s then austenitized for 1 minute followed by cooling to room temperature at the cooling rates of 0.3 °C/s, 1 °C/s, and 5 °C/s, respectively. Since the evolution of microstructural bands is known to be sensitive to the cooling rate after austenitization,^[14] those cooling rates were adopted to investigate the evolution of microstructural bands during austenite decomposition and its effect on the dilatation behavior.

The specimens for metallographic analysis were prepared using standard methods. The microstructure after the thermal cycle was observed with a light microscope using 2 pct nital etchant. The fraction of ferrite and pearlite was measured using a quantitative image analysis software.

Figure 2 shows the dilatometric curves measured under given cooling rates. When the cooling rate is 0.3 °C/s, the dilatation behavior is strongly dependent on the specimen orientation. The length change of the ND specimen when cooled is greater than that of the RD specimen, and the difference is approximately 34 μ m when the transformation is completed. However, the orientation dependence is diminished as the cooling rate is increased, and similar dilatation behavior is observed with a cooling rate of 5 °C/s. Figure 3 shows the microstructures of dilatometric specimens after completing the thermal cycle. The microstructural bands are well developed with a cooling rate of 0.3 °C/s, but their aspect ratio is decreased as the cooling rate is increased to 1 °C/s. Further, the microstructural bands completely disappear when the cooling rate is 5 °C/s. The microstructures in Figure 3 agree with the earlier article, which reported that a cooling rate faster than 1 °C/s prevented the evolution of microstructural bands.^[14] The accelerated cooling was believed to increase the driving force for nucleation of proeutectoid ferrite, which enabled ferrite to nucleate randomly despite the banded region, with the segregation of substitutional alloying elements. Table II summarizes the phase fraction measured with a quantitative image analysis. The pearlite fraction is comparable to the equilibrium fraction when the cooling rate is 0.3 °C/s, but it is slightly increased with an acceleration of the cooling rate. The increase of the pearlite fraction with the acceleration of the cooling rate is attributed to the lower transformation temperature, which causes the pearlite transformation to be triggered with less carbon enrichment in austenite.^[12]

The dilatation behavior and corresponding microstructural evolution in Figures 2 and 3 show that the orientation dependence of dilatation behavior is accompanied by the occurrence of microstructural bands, which implies a close relationship between them. It indicates that the effect of the microstructural directionality on the dilatation behavior should be taken into account for the quantitative dilatometric analysis of austenite decomposition.

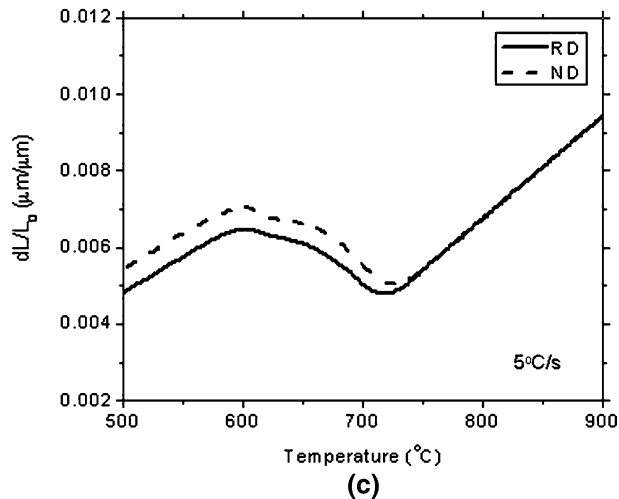
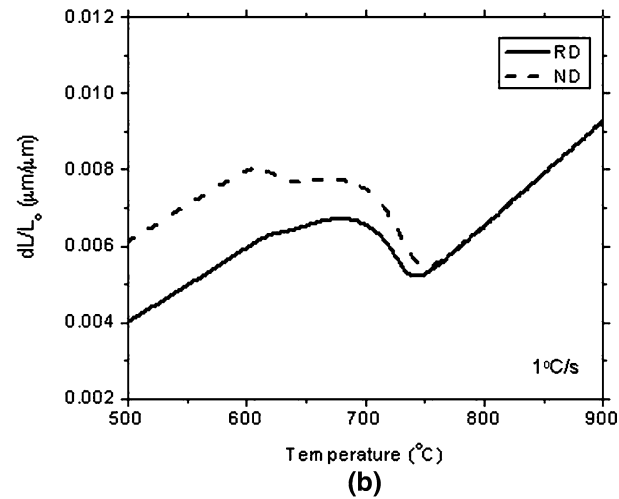
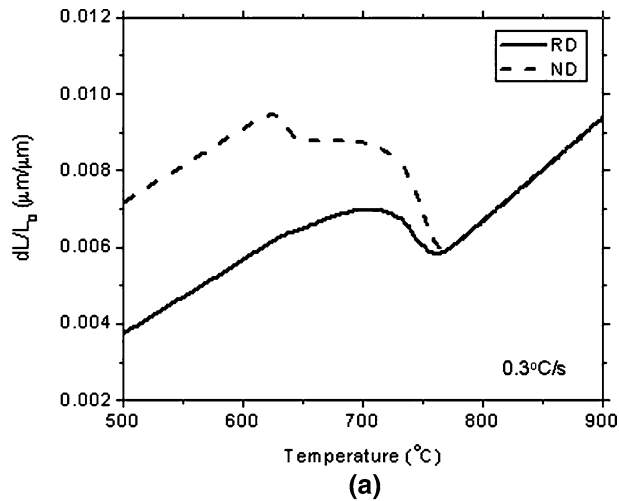


Fig. 2—Dilatation curves of RD and ND specimens upon cooling. (a) Cooling rate of 0.3 °C/s. (b) Cooling rate of 1 °C/s. (c) Cooling rate of 5 °C/s.

III. DILATOMETRIC ANALYSIS PROCEDURE

As mentioned, several types of dilatometric analysis models have been suggested, but it has rarely been

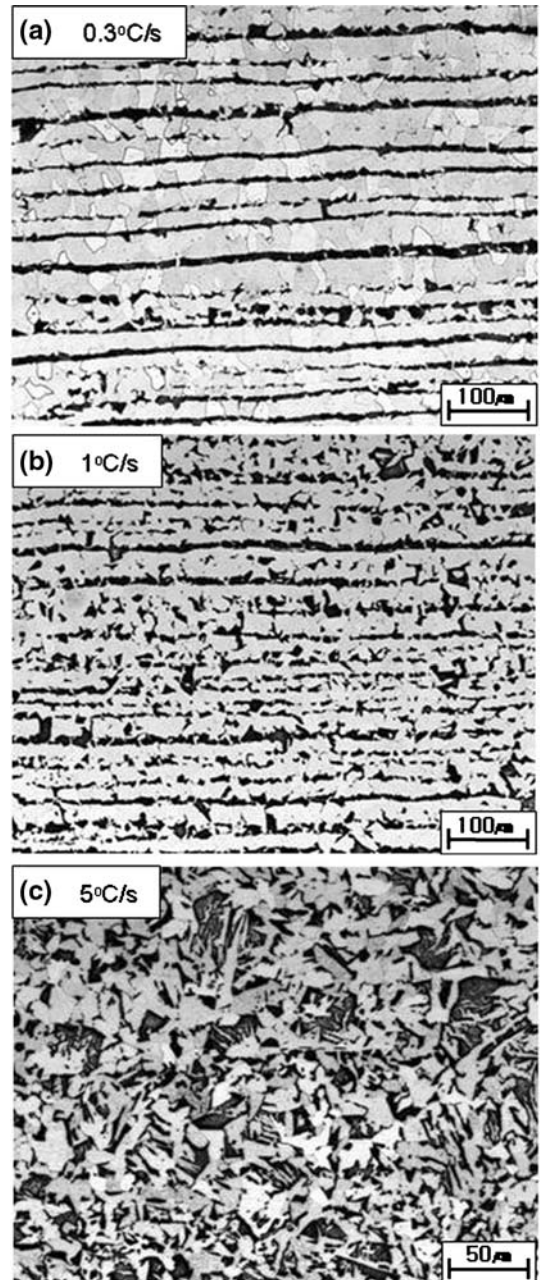


Fig. 3—Microstructures after thermal cycle for dilatation measurement. (a) Cooling rate of 0.3 °C/s. (b) Cooling rate of 1 °C/s. (c) Cooling rate of 5 °C/s.

Table II. Phase Fraction of Pearlite after the Thermal Cycle

Cooling Rate (°C/s)	0.3	1	5
Measured fraction	0.217 ± 0.025	0.224 ± 0.022	0.253 ± 0.031
Equilibrium fraction	0.204		

verified whether they are applicable to the dilatometric curves showing orientation dependence due to the microstructural directionality. In this article, first the

reliability of the phase fraction as evaluated from the conventional lever rule is examined, and then a dilatometric analysis procedure is proposed, which considers the effect of the microstructural directionality on the dilatation behavior.

A. Dilatometric Analysis with the Lever Rule

The lever rule is the simplest method to extract the transformed fraction from the dilatation data.^[1] The dilatometric curve shows linear thermal expansion characteristics in the temperature range where no transformation occurs. In the lever rule, two linear segments in dilatometric curve are extrapolated, and the fraction of the transformed phase at a given temperature is evaluated by the relative position of the measured dilatometric curve between both extrapolated lines. Figure 4 presents the phase fractions from the dilatometric curves in Figure 2 using the lever rule. For a cooling rate of 5 °C/s, the phase fractions from the RD and ND specimens show a reasonable agreement with each other because the microstructural bands are not developed and thus the orientation dependence of the dilatometric curves are not remarkable. However, the phase fractions by the lever rule are considerably different between the RD and ND specimens cooled at 0.3 °C/s and 1 °C/s. Even though the transformation starting and ending temperatures can be consistently determined, the difference of the transformation kinetics between the RD and ND specimens becomes significant with the evolution of the microstructural bands. Since the transformation kinetics do not have orientation dependence under a given thermal history, the analysis results in Figure 4 indicate that the reliable phase fraction is difficult to obtain by the lever rule when the microstructural directionality affects the dilatation behavior.

B. Dilatometric Analysis Considering the Effect of Microstructural Directionality

The overall volume change associated with the transformation should be the same under a given thermal cycle. It means that the orientation dependence of dilatation behavior in Figure 2 originates from the nonisotropic volume change during the transformation. The effect of nonisotropic volume change on the dilatation data can be quantified by specifying the nonisotropic dilatation from the dilatometric curve. Figure 5 shows the dilatometric curves of the RD and ND specimens cooled at 0.3 °C/s. Let us assume that the dotted line exhibits the thermal expansion behavior of hypothetical ferrite-pearlite, which is transformed from austenite under isotropic volume change. Thus, the overall nonisotropic dilatation of the RD and ND specimens are represented as Δ_2^{RD} and Δ_2^{ND} from the definition of nonisotropic dilatation on cooling.^[12]

To take into account the nonisotropic dilatation in the dilatometric analysis procedure, we first examine the

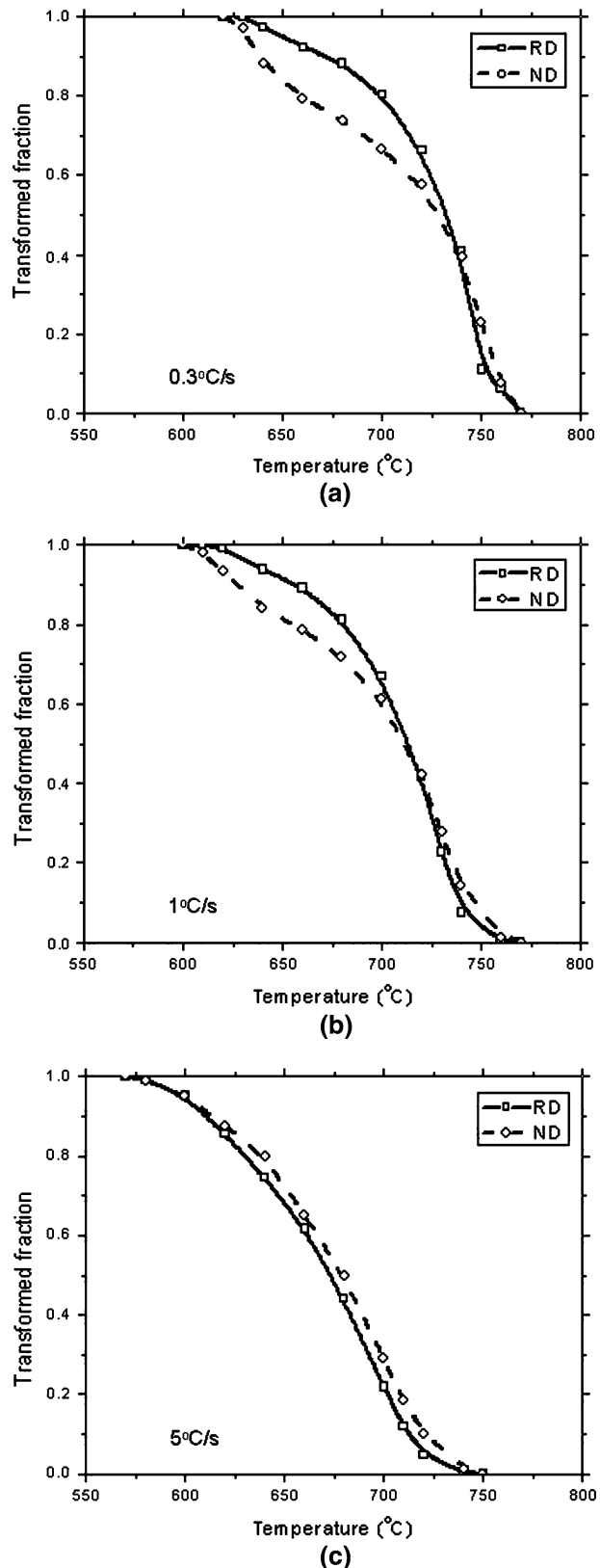


Fig. 4—Phase fraction during austenite decomposition upon cooling from lever rule. (a) Cooling rate of 0.3 °C/s. (b) Cooling rate of 1 °C/s. (c) Cooling rate of 5 °C/s.

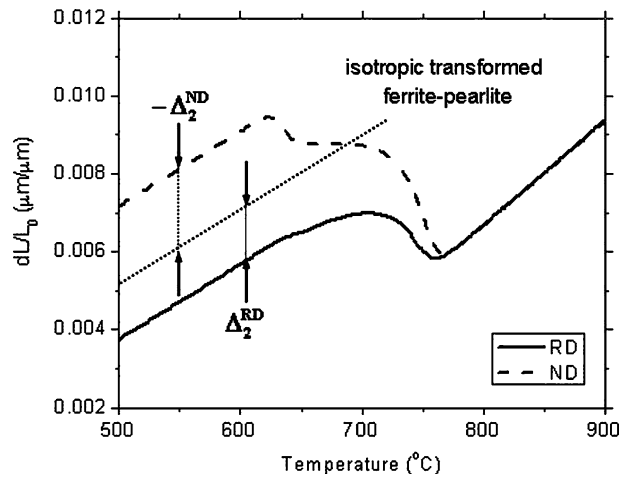


Fig. 5—Overall nonisotropic dilatation of RD and ND specimens with cooling rate of 0.3 °C/s.

origin of the nonisotropic dilatation in the microstructurally-banded specimen. The earlier articles reported that the deformation behavior described as transformation plasticity was responsible for the dimensional change of the specimen upon the thermal cycle.^[11,19,20] Transformation plasticity is a phenomenon where a permanent strain remains after the phase transformation when the transformation proceeds under external stress even lower than the yield strength. Several mechanisms have been suggested to interpret this phenomenon. The “Magee mechanism”^[19] considered the selection of an energetically favorable variant under external stress. On the other hand, the “Greenwood–Johnson mechanism”^[20] is associated with the plastic deformation of a weaker phase to accommodate the external and internal stress that are caused by volume change during the phase transformation. Besides, Han *et al.*^[21] suggested a diffusion-controlled model reflecting *in-situ* microstructural observation of transformation plasticity in iron. It was recently reported that transformation plasticity brings about nonisotropic dilatation even for a homogeneous microstructure, which is not subjected to the external stress during the thermal cycle.^[12,17,18] For a homogeneous microstructure without external stress, it is believed that the radial thermal gradient due to the specimen geometry encourages the propagation of the phase boundary along the radial direction during transformation, and the directional movement of the phase boundary generates the nonisotropic strain. The dilatometric analysis considering the geometric effect was successfully applied to the evaluation of the phase fraction during austenite decomposition with homogeneous microstructure.^[12] The geometric effect will also exist in a specimen with a microstructural directionality. However, given that it depends on the specimen geometry, the geometric effect cannot generate the orientation dependence of the nonisotropic dilatation. Therefore, the dilatation behavior showing orientation dependence should be brought about by another source, which is associated with the microstructural directionality.

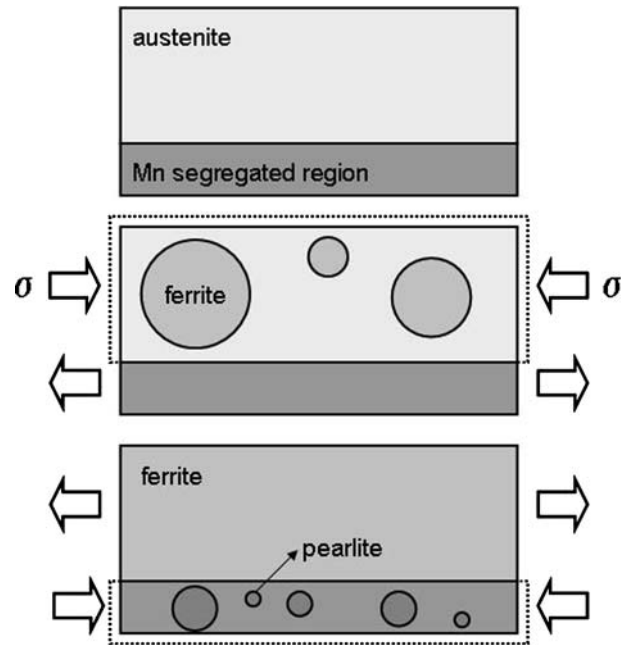


Fig. 6—Schematic representation of apparent stress evolution originating from microstructural directionality.

Figure 6 schematically describes the evolution of apparent stress due to the microstructural bands, which possibly induces the nonisotropic dilatation along a specific specimen orientation. In Figure 6, Mn is shown as a major substitutional alloying element responsible for the microstructural bands due to making up the greatest part of the investigated alloy. When austenite-to-ferrite transformation proceeds during cooling, the ferrite will preferentially form at the Mn lean layer because Mn is an austenite stabilizer that decreases A_{r3} temperature. Since the ferrite has a larger atomic volume than the austenite, the layer where ferrite transformation proceeds is subject to compressive stress along the banded direction to maintain compatibility with neighboring layers. Similarly, when the pearlite transformation proceeds at the Mn-rich layer after completing the ferrite transformation, the layer is also exposed to compressive stress because of the atomic volume difference of austenite and pearlite. In this way, the transforming layer is subjected to the compressive stress along the banded direction through the transformation. The compressive stress will generate the transformation plasticity along the banded direction. For the RD specimen, the banded direction is parallel to the axial direction along which the length change of the specimen is monitored. Therefore, the dilatometric specimen expands less than that expected under the isotropic volume change along the axial direction. On the other hand, given that the banded direction is parallel to the radial direction for the ND specimen, the dilatometric specimen expands less than expected under isotropic volume change along the radial direction, which leads to additional extension along the axial direction. In this case, the nonisotropic dilatation is dependent on the specimen orientation, and thus the dilatation behavior

will show orientation dependence. Note that the geometric effect also occurs during the thermal cycle regardless of the degree of microstructural directionality. Therefore, overall nonisotropic dilatation for a specimen with microstructural bands will be governed by both geometric and microstructural effects.

Assuming that the transformation plasticity from the geometric and microstructural effects independently generates the nonisotropic dilatation, the overall nonisotropic dilatation is given by

$$\begin{aligned}\Delta_2^{\text{RD}} &= \Delta_g + \Delta_m^{\text{RD}} \\ \Delta_2^{\text{ND}} &= \Delta_g + \Delta_m^{\text{ND}}\end{aligned}\quad [1]$$

where Δ_g and Δ_m represent the nonisotropic dilatation from the geometric and the microstructural effect, respectively. The nonisotropic dilatation from the geometric effect, Δ_g , is assumed to be the same for the RD and ND specimens because of the equivalent geometry.

Since Δ_m^{RD} and Δ_m^{ND} are related to the shape change of the simple description of the microstructurally banded structure, as shown in Figure 7:

$$L^3 - (L - \Delta_m^{\text{RD}}) \cdot (L - \Delta_m^{\text{RD}}) \cdot (L - \Delta_m^{\text{ND}}) = 0 \quad [2]$$

the following relation is obtained when the terms higher than the second order are ignored:

$$2 \cdot \Delta_m^{\text{RD}} + \Delta_m^{\text{ND}} = 0 \quad [3]$$

By combining Eqs. [1] and [3], the nonisotropic dilatations from the microstructural effect and the geometric effect can be expressed as follows:

$$\begin{aligned}\Delta_g &= \frac{1}{3}(2 \cdot \Delta_2^{\text{RD}} + \Delta_2^{\text{ND}}) \\ \Delta_m^{\text{RD}} &= \frac{1}{3}(\Delta_2^{\text{RD}} - \Delta_2^{\text{ND}}), \quad \Delta_m^{\text{ND}} = -\frac{2}{3}(\Delta_2^{\text{RD}} - \Delta_2^{\text{ND}})\end{aligned}\quad [4]$$

Equation [4] indicates an accumulated nonisotropic dilatation as a result of the complete decomposition of austenite. For implementation of these nonisotropic dilatations into the dilatometric analysis procedure,

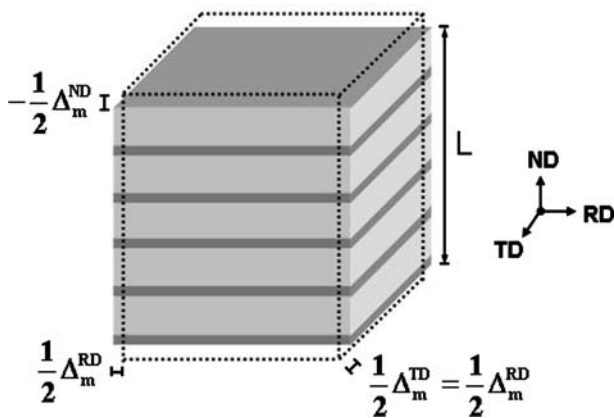


Fig. 7—Simple description of microstructurally banded structure and shape change from nonisotropic dilatation.

it is necessary to formulate the evolution of the nonisotropic dilatation with the progress of the transformation.

In their article on the generalization of the Greenwood–Johnson model, Schuh *et al.* have formulated the strain rate of transformation plasticity with the progress of the transformation.^[22] If the weaker phase is deformed through yielding, the strain rate is given by

$$\dot{\varepsilon} = \frac{5}{6} \cdot \frac{\sigma}{\sigma_Y} \cdot \left| \frac{\Delta V}{V} \right| \cdot \dot{f} \quad [5]$$

where σ_Y is the yield stress of the weaker phase, σ is the external stress, $|\Delta V/V|$ is the volume mismatch, and \dot{f} is the time derivative of the transformed phase fraction. From Eq. [5], the authors assumed that the nonisotropic dilatation from the geometric effect would be linearly increased with the progress of the austenite decomposition associated with homogeneous microstructure.^[12] In this study, the evolution of nonisotropic dilatation from the geometric effect is also assumed to have a linear relationship with the transformed fraction as follows:

$$\underline{\Delta}_g = \Delta_g \cdot (f^{\alpha} + f^{\beta}) \quad [6]$$

The underbar indicates the nonisotropic dilatation during the transformation.

Next, let us consider the evolution of nonisotropic dilatation from the microstructural effect. As shown in Figure 6, the apparent compressive stress on the transforming layer is generated by the volume mismatch between the parent and the transformed phase. Since the ferrite and pearlite have dissimilar atomic volumes, the level of apparent stress due to the volume mismatch with austenite will be different. Given that the strain rate of transformation plasticity is dependent on the level of apparent stress as well as the volume mismatch itself in Eq. [5], the nonisotropic strain per unit of transformed fraction of ferrite and pearlite will be different. It is therefore necessary to distinguish the contribution of individual transformation to the evolution of nonisotropic dilatation from the microstructural effect. In that case, assuming the linear relationship between the amount of nonisotropic dilatation and the fraction of transformed phase for the individual transformation, a pair of linear relationships with different slopes can describe the evolution of nonisotropic dilatation during the entire transformation, as shown in Figure 8. The constants k_1 and k_2 in Figure 8 represent the relative contributions of ferrite and pearlite transformation to the evolution of nonisotropic dilatation. The nonisotropic dilatation from the microstructural effect does not increase linearly with the total fraction of the transformed phase, even though it has a linear relationship with the transformed fraction during the individual transformation. Then the nonisotropic dilatation from the microstructural effect during ferrite transformation is given by

$$\underline{\Delta}_m^i = \Delta_m^i \cdot (k_1 \cdot f^{\alpha}) \quad [7]$$

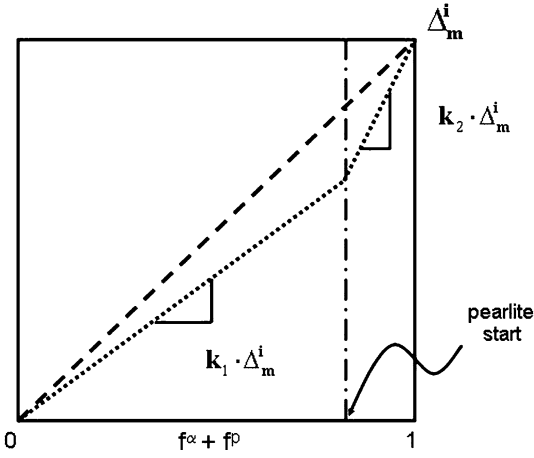


Fig. 8—Evolution of nonisotropic dilatation from microstructural effect as a function of fraction of transformed phase.

and it is given in the following form for pearlite transformation:

$$\begin{aligned}\Delta_m^i &= \Delta_m^i \cdot (k_1 \cdot f^\alpha + k_2 \cdot f^p) \\ &= \Delta_m^i \cdot \left[k_1 \cdot f^\alpha + \left(\frac{1 - k_1 \cdot f^\alpha}{1 - f^\alpha} \right) \cdot f^p \right]\end{aligned}\quad [8]$$

The superscript i represents the specimen orientation, RD or ND.

Combining Eqs. [6] through [8] yields the nonisotropic dilatation during the austenite decomposition from the geometric and microstructural effects:

$$\begin{aligned}\underline{\Delta}_2^i &= \Delta_m^i \cdot \left[k_1 \cdot f^\alpha + \left(\frac{1 - k_1 \cdot f^\alpha}{1 - f^\alpha} \right) \cdot f^p \right] + \Delta_g \cdot (f^\alpha + f^p) \\ &= (k_1 \cdot \Delta_m^i + \Delta_g) \cdot f^\alpha + \left[\left(\frac{1 - k_1 \cdot f^\alpha}{1 - f^\alpha} \right) \cdot \Delta_m^i + \Delta_g \right] \cdot f^p\end{aligned}\quad [9]$$

The description of the nonisotropic dilatation in Eq. [9] allows the isotropic dilatation during the phase transformation to be represented as follows:

$$\begin{aligned}\Delta L_{\text{iso}}^i &= \Delta L_{\text{exp}}^i + \underline{\Delta}_2^i \\ &= \Delta L_{\text{exp}}^i + (k_1 \cdot \Delta_m^i + \Delta_g) \cdot f^\alpha \\ &\quad + \left[\left(\frac{1 - k_1 \cdot f^\alpha}{1 - f^\alpha} \right) \cdot \Delta_m^i + \Delta_g \right] \cdot f^p \\ &= \Delta L_{\text{exp}}^i + D_1 \cdot f^\alpha + D_2 \cdot f^p\end{aligned}\quad [10]$$

$$\left(D_1 = k_1 \cdot \Delta_m^i + \Delta_g, \quad D_2 = \left(\frac{1 - k_1 \cdot f^\alpha}{1 - f^\alpha} \right) \cdot \Delta_m^i + \Delta_g \right)$$

Equation [10] represents a formulation of the isotropic dilatation that compensates for the nonisotropic dilatation from the microstructural effect as well as the geometric one. Therefore, the phase fraction involved with the transformation can be evaluated by the implementation of Eq. [10] into the dilatometric analysis model proposed by the authors.^[12]

C. Determination of Nonisotropic Dilatation and Constant k_1

For evaluating the phase fraction by Eq. [10], the value of Δ_g , Δ_m^i and k_1 should be determined. In our previous article, we proposed a method to evaluate the overall nonisotropic dilatation (Δ_2^i) by performing an iterative calculation of the phase fraction until the phase fraction after completing the transformation and the nonisotropic dilatation converge on values that are compatible with each other. The same procedure is adopted in this study to estimate the nonisotropic dilatation, Δ_2^{RD} and Δ_2^{ND} , from each dilatometric curve of the RD and ND specimens. After the overall nonisotropic dilatation is obtained, the contribution of the microstructural and geometric effects is evaluated from Eq. [4].

When the Δ_g and Δ_m^i are available, we can obtain a pair of phase fractions for a given value of k_1 from the analysis of the dilatometric curve of the RD and ND specimens. Considering that the phase fractions of the RD and ND specimens should be coincident under the same thermal cycle, the constant k_1 is determined by adjusting the value until the best match between the phase fractions evaluated from the RD and ND specimens is obtained.

IV. ANALYSIS, RESULTS, AND DISCUSSION

A. Nonisotropic Dilatation

Figure 9(a) shows the overall nonisotropic dilatation after the completion of the transformation evaluated from the proposed dilatometric analysis. The orientation dependence of the nonisotropic dilatations is remarkable at a cooling rate of 0.3 °C/s, but it gradually disappears as the cooling rate increases. Assuming that the total nonisotropic dilatations consist of those from the geometric and microstructural effects, the contribution of individual effects can be evaluated from Eq. [4]. Figure 9(b) indicates the contribution of the nonisotropic dilatation from the microstructural and geometric effects. The nonisotropic dilatation from the microstructural effect is gradually decreased with the acceleration of the cooling rate, but that from the geometric effect is gradually increased, and in fact is expected from the origins of each nonisotropic dilatation. Since the increase in cooling rate suppresses the evolution of microstructural bands as shown in Figure 3, the microstructural effect on the evolution of nonisotropic dilatation will be decreased by the acceleration of the cooling rate. On the other hand, increasing the cooling rate encourages the evolution of nonisotropic dilatation from the geometric effect because it will promote the temperature gradient in the dilatometric specimen. It is noted in Figure 9(b) that the microstructural effect dominates the evolution of nonisotropic dilatation at slow cooling rates where the microstructural bands are developed, but the geometric effect becomes more remarkable when the microstructural directionality diminishes.

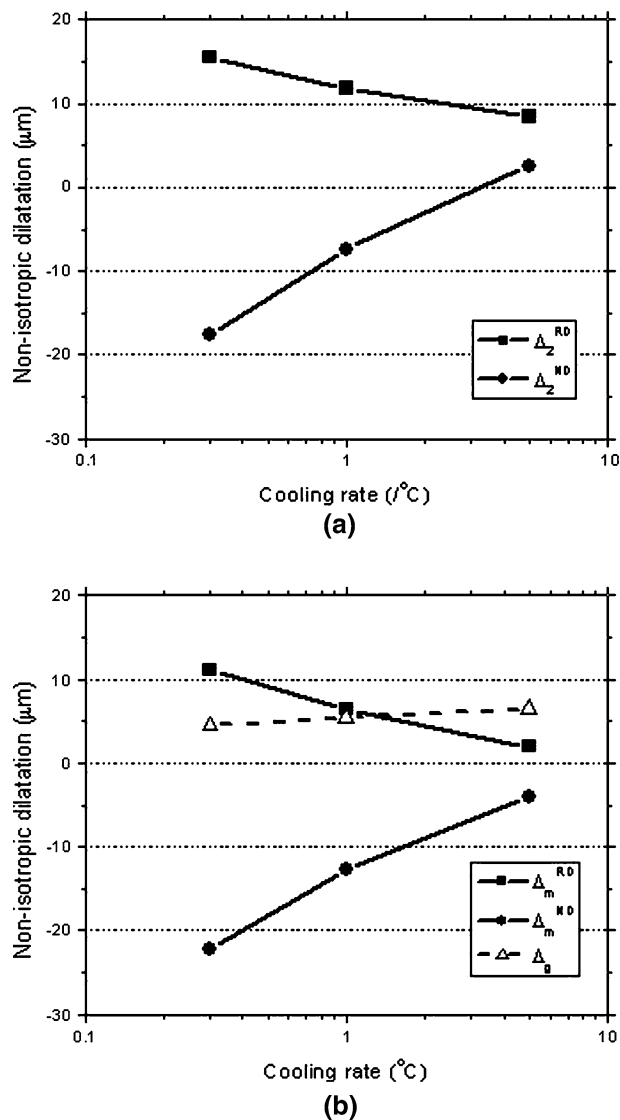


Fig. 9—Nonisotropic dilatation according to the cooling rate. (a) Overall nonisotropic dilatation. (b) Nonisotropic dilatation from geometric and microstructural effect.

Table III. Difference between Overall NonIsotropic Dilatation of RD and ND Specimens

Cooling Rate (°C)	$(\Delta_2^{RD} - \Delta_2^{ND})$, in μm	
	Dilatometric	Graphical
0.3	33.3	33.9
1	19.2	20.9
5	5.89	6.10

The difference between the overall nonisotropic dilatation of the RD and ND specimens, $(\Delta_2^{RD} - \Delta_2^{ND})$, graphically corresponds to the interval between both dilatometric curves as shown in Figure 5. Table III compares the difference between overall nonisotropic dilatations, which are calculated with the dilatometric and graphical analysis, respectively. The difference between the overall nonisotropic dilatation between

the RD and ND specimens from dilatometric analysis is consistent with that from the graphical analysis. It confirms that the analysis for the individual dilatometric curve yields overall nonisotropic dilatation of the RD and ND specimens, which are compatible with each other.

B. Dilatometric Analysis Considering Nonisotropic Effect

Equation [10] presents a formulation of the isotropic dilatation that compensates for the contribution of the nonisotropic effect, and thus its implementation into the dilatometric analysis procedure allows evaluation of the phase fraction for a given value of k_1 . As mentioned, the constant k_1 is optimized to minimize the sum of squared differences between the phase fractions evaluated from the RD and ND specimens. The constant k_1 is optimized to be 0.80 and 0.81 for a cooling rate of 0.3 °C/s and 1 °C/s, respectively. Figures 10(a) and (b) show the phase fractions evaluated from the proposed dilatometric analysis procedure. Compared with the analysis results from the lever rule, the phase fractions of the RD and ND specimens from the proposed procedure show reasonable agreement with each other. For a cooling rate of 5 °C/s, according to the decrease of the nonisotropic dilatation from the microstructural effect, the analysis result is not sensitive to the variation of the constant k_1 . Figure 10(c) shows analysis results with the k_1 of 1.0. In Figure 10, symbols represent the phase fraction after completing the transformation measured by a metallographic analysis. The phase fraction by proposed dilatometric analysis agrees with the metallographically analyzed one. It demonstrates that the dilatometric analysis suggested in this article gives a reliable phase fraction even for the dilatometric curves showing orientation dependence due to the microstructural bands.

The importance of considering the nonisotropic effect can be confirmed by comparing the pearlite transformation start temperature predicted by the suggested dilatometric analysis with that predicted by the conventional lever rule. Table IV shows the comparison between the pearlite start temperatures evaluated from both the lever rule and the dilatometric analysis procedure. To determine the pearlite start temperature by the lever rule, the measured pearlite fractions in Table II have been used. The pearlite transformation start temperature estimated from the inflection point on the dilatometric curve is also presented for comparison. Table IV indicates that the pearlite start temperature from the lever rule is considerably affected by the specimen orientation. The difference between the RD and ND specimens increases as the cooling rate is decreased, while the formation of microstructural bands is enhanced. Compared with the inflection point, the pearlite start point from the lever rule is higher, especially for the RD specimen. On the other hand, the proposed dilatometric analysis consistently predicts the pearlite start temperatures regardless of the specimen orientation. Further, the pearlite start points from the proposed analysis show reasonable agreement with

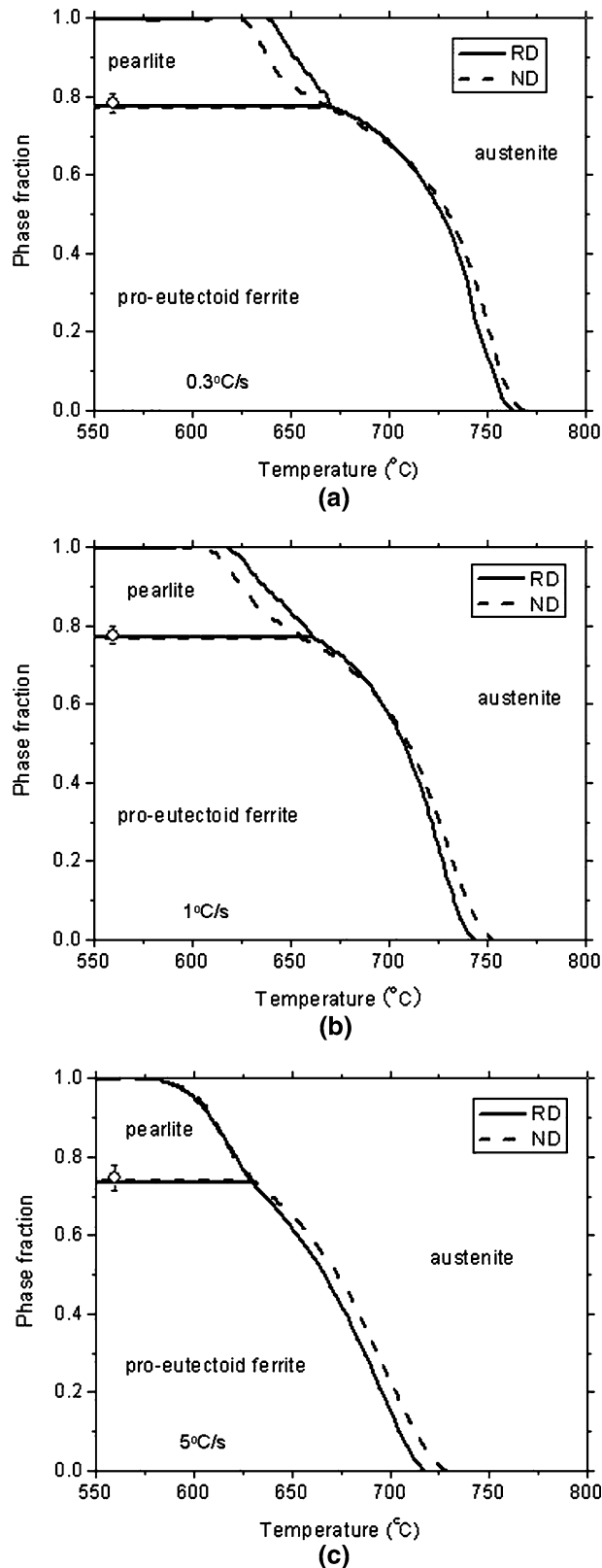


Fig. 10—Phase fraction during austenite decomposition upon cooling with proposed dilatometric analysis. (a) Cooling rate of 0.3 °C/s. (b) Cooling rate of 1 °C/s. (c) Cooling rate of 5 °C/s.

Table IV. Pearlite Transformation Start Temperature (°C)

Cooling Rate		Conventional Lever Rule	Dilatometric Analysis	Inflection Point
0.3 °C	RD	702	672	666
	ND	665	670	662
1 °C	RD	684	662	656
	ND	663	658	658
5 °C	RD	647	630	635
	ND	639	631	633

the inflection points. This suggests that systematic implementation of the nonisotropic dilatation into dilatometric analysis is critical for the quantitative evaluation of the transformation kinetics.

In the present study, the constants k_1 and k_2 describe the relative contributions of ferrite and pearlite transformation to the evolution of nonisotropic dilatation from the microstructural effect. The value of k_1 less than 1 implies that the evolution rate of nonisotropic dilatation per unit of transformed fraction of ferrite is slower than that of pearlite. According to the Eq. [5], the strain rate of transformation plasticity is increased with the increment of the applied stress and the volume mismatch. Given that the volume mismatch between phases plays a major role in generating the apparent stress, the evolution of nonisotropic dilatation from the microstructural effect will be accelerated as the volume mismatch increases. A comparison of the volume mismatch between austenite and ferrite with that between austenite and pearlite is not straightforward because the atomic volume of each phase varies as a function of temperature or solute carbon content. However, the weighted average of volume mismatch along the transformation can be evaluated from the change of volume mismatch as follows:

$$\left| \frac{\Delta V}{V} \right|_i = \frac{\int_0^{V_i} \left| \frac{\Delta V}{V} \right|_i \cdot dV}{V_i} \quad [11]$$

where subscript i represents the ferrite or pearlite phase, $|\Delta V/V|_i$ is the volume mismatch with austenite, and V_i is the final phase fraction. Figure 11 shows the change of volume mismatch when considering the effect of carbon enrichment in austenite, as well as the temperature dependence of atomic volume in the case of austenite decomposition with a cooling rate of 0.3 °C/s. It indicates that the volume mismatch between austenite and ferrite is greater than that between austenite and pearlite at an earlier stage of ferrite formation, but the mismatch becomes less than that between austenite and pearlite due to the carbon enrichment in austenite's gradually decreasing the difference of atomic volume between austenite and ferrite. The $|\Delta V/V|_{ferrite}$ and $|\Delta V/V|_{pearlite}$ is evaluated as 0.0073 and 0.0082. The greater average volume mismatch between austenite and pearlite than that between austenite and ferrite possibly suggests that the evolution of nonisotropic dilatation

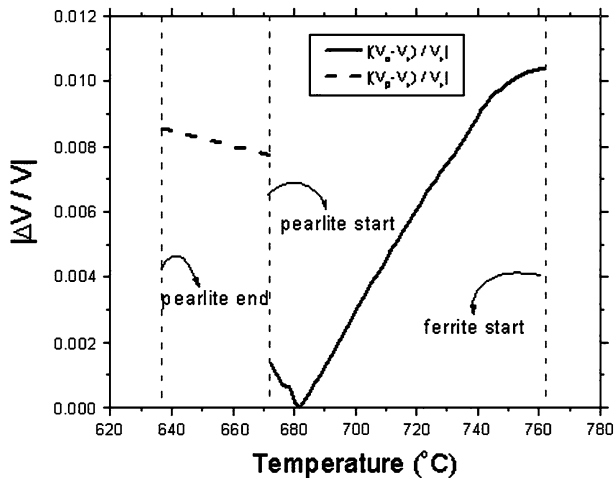


Fig. 11—Atomic volume mismatch between austenite and ferrite, and that between austenite and pearlite in the case of austenite decomposition with a cooling rate of 0.3 °C/s.

would be promoted more during the pearlite transformation, which agrees with the optimized value of k_1 of less than 1 in this study. However, it should be noted that the volume mismatches vary considerably with the progress of transformation, and therefore further investigation is necessary to quantify its effect on the evolution rate of nonisotropic dilatation.

C. Limit of the Present Analysis Procedure

The dilatometric analysis proposed in this article predicts the final phase fraction measured from metallographic analysis with reasonable accuracy, even for the dilatometric curves showing orientation dependence. However, it is noted that some disagreement still remains between the transformation kinetics evaluated from the RD and ND specimens. The disagreement possibly originates from the following limit of present analysis procedure.

The schematic description of a microstructurally banded structure and the evolution of apparent stress due to the microstructural directionality are significantly simplified in the present study. Based on the schematic modeling, the apparent stress is assumed to be constant during the transformation. However, in real microstructure, the microstructural bands are far more complicated than a simple alternating layer of ferrite and pearlite. The evolution of apparent stress along the banded direction, therefore, is not the same for the whole volume of the specimen, which affects the evolution rate of the nonisotropic dilatation. Besides, the proposed analysis assumes a linear evolution of the nonisotropic dilatation with respect to the transformed fraction of ferrite and pearlite. This simplification neglects the temperature dependence of the apparent stress induced by the volume mismatch. The temperature dependence of the apparent stress can lead to a nonlinear evolution of the nonisotropic dilatation, which is not taken into account in the proposed dilatometric analysis.

V. CONCLUSIONS

This article is intended to propose a dilatometric analysis of austenite decomposition in low-carbon steel, which shows distinct dilatation behavior with the specimen orientation due to the microstructural directionality. Measured dilatometric curves of low-carbon steel showing microstructural bands are analyzed and the following conclusions can be drawn.

1. The evolution of microstructural bands during the transformation significantly affects the dilatation behavior depending on the specimen orientation. With well-developed microstructural bands, distinctly different dilatation behaviors are observed according to the specimen orientation, but the orientation dependence vanishes as the microstructural bands disappear.
2. The orientation dependence of dilatation behavior is associated with nonisotropic dilatation originating from the microstructural directionality. The microstructural and geometric effects on the evolution of the nonisotropic dilatation are quantified, and implemented into the dilatometric analysis procedure.
3. The dilatometric curves of low-carbon steel showing microstructural bands are analyzed with the conventional lever rule and the dilatometric analysis proposed in the present study. It is difficult to extract quantitative phase fractions from the orientation-dependent dilatometric curves by the lever rule. However, the proposed analysis procedure permits a reliable evaluation of phase fractions, which agree with the metallographic analysis results.

ACKNOWLEDGMENTS

The authors acknowledge the Korean Government (MOCIE) for its financial support. One of the authors (HNH) also thanks the Korea Science and Engineering Foundation (KOSEF) for Grant No. R0A-2007-000-10014-0, which was funded by the Korean government (MOST).

REFERENCES

1. *ASTM International*, Designation: A 1033-04, 2004, pp. 1–14.
2. M. Takahashi and H.K.D.H. Bhadeshia: *J. Mater. Sci. Lett.*, 1989, vol. 8, pp. 477–78.
3. C. García de Andrés, F.G. Caballero, and C. Capdevila: *Scripta Mater.*, 1998, vol. 38, pp. 1835–42.
4. R.C. Dykhuizen, C.V. Robino, and G.A. Knorovsky: *Metall. Mater. Trans. B*, 1999, vol. 30B, pp. 107–17.
5. C. García de Andrés, F.G. Caballero, C. Capdevila, and L.F. Álvarez: *Mater. Characterization*, 2002, vol. 48, pp. 101–11.
6. J. Huang, W.J. Poole, and M. Milizer: *Metall. Mater. Trans. A*, 2004, vol. 35A, pp. 3363–75.
7. J. Zhao, C. Mesplont, and B.C. De Cooman: *Mater. Sci. Eng., A*, 2002, vol. A332, pp. 110–16.
8. H.N. Han, J.K. Lee, S.H. Park, and K.J. Lee: *J. Kor. Inst. Met. Mater.*, 2000, vol. 38, pp. 409–13.

9. S. Choi: *Mater. Sci. Eng., A*, 2003, vol. A363, pp. 72–80.
10. C.S. Oh, H.N. Han, C.G. Lee, T.H. Lee, and S.J. Kim: *Met. Mater. Int.*, 2004, vol. 10, pp. 399–406.
11. T.A. Kop, J. Sietsma, and S. Van Der Zwaag: *J. Mater. Sci.*, 2001, vol. 36, pp. 519–26.
12. D.W. Suh, C.S. Oh, H.N. Han, and S.J. Kim: *Acta Mater.*, 2007, vol. 55, pp. 2659–69.
13. R.G. Ward: *JISI*, 1965, vol. 203, pp. 930–32.
14. S.W. Thompson and P.R. Howell: *Mater. Sci. Technol.*, 1992, vol. 8, pp. 777–84.
15. R.A. Grange: *Metall. Trans.*, 1971, vol. 2, pp. 417–26.
16. T.A. Kop, J. Sietsma, and S. Van Der Zwaag: *Mater. Sci. Technol.*, 2001, vol. 17, pp. 1569–74.
17. R.A. Jaramillo, M.T. Lusk, and M.C. Mataya: *Acta Mater.*, 2004, vol. 52, pp. 851–58.
18. R.A. Jaramillo and M.T. Lusk: *Acta Mater.*, 2004, vol. 52, pp. 859–67.
19. C.L. Magee and H.W. Paxton: *Trans. Met. Soc. AIME*, 1968, vol. 242, pp. 1741–49.
20. G.W. Greenwood and R.H. Johnson: *Proc. R. Soc. A*, 1965, vol. 283, pp. 403–22.
21. H.N. Han, J.K. Lee, D.W. Suh, and S.J. Kim: *Philos. Mag.*, 2007, vol. 87, pp. 159–76.
22. C. Schuh and D.C. Dunand: *Acta Mater.*, 2001, vol. 49, pp. 199–210.